

## Structure–Property Correlation of CdSe Clusters Using Experimental Results and First-Principles DFT Calculations

Rajan Jose,<sup>†</sup> Nurbosyn U. Zhanpeisov,<sup>\*,‡</sup> Hiroshi Fukumura,<sup>‡</sup>  
Yoshinobu Baba,<sup>†,§</sup> and Mitsuru Ishikawa<sup>†</sup>

Contribution from the Nano-bioanalysis Team, Health Technology Research Center, National Institute of Advanced Industrial Science and Technology, 2217-14 Hayashi Cho, Takamatsu, Kagawa 761-0395, Japan, Department of Chemistry, Graduate School of Science, Tohoku University, Aramaki-Aoba, Aoba-ku, Sendai 980-8578, Japan, and Department of Applied Chemistry, Graduate School of Engineering, Nagoya University, Japan

Received September 28, 2005; E-mail: nurbosyn@orgphys.chem.tohoku.ac.jp

**Abstract:** Structures and properties of CdSe quantum dots (clusters) up to a diameter of ~2 nm were investigated by combining experimental absorption, photoluminescence (PL), and X-ray diffraction (XRD) spectroscopies as well as ab initio DFT calculations. These CdSe clusters were nucleated and grown from solutions containing respective cadmium and selenium precursors following the hot-injection technique that allows one to obtain size-controlled CdSe clusters having PL efficiency up to 0.5. The DFT calculations were performed at the B3LYP/Lanl2dz level and followed by time-dependent TDDFT calculations to estimate the energy singlet transitions. On the basis of the results of these experimental and theoretical studies, an approach to determine whether the proposed cluster with a mean diameter of ~2 nm is more physically reasonable is discussed. It was shown that the minimum nucleus of a CdSe cluster consists of (CdSe)<sub>3</sub> with a six-membered ring and planar structure. No PL is observed for this structure. The formation of the next stable cluster depends on whether hexadecylamine (HDA) was used for the growth of the CdSe clusters. In the absence of HDA, the second cluster was found to be (CdSe)<sub>6</sub> characterized by a broad PL spectrum, while in the presence of HDA, it was found to be (CdSe)<sub>n</sub> (where  $n \geq 14$ ) with a sharp PL spectrum.

### Introduction

Advances in the synthesis of CdSe quantum dots (QDs) through controlled colloidal processing<sup>1–3</sup> and understanding of the factors that control  $\Phi_{\text{PL}}$  of CdSe QDs<sup>4–11</sup> enabled us to find technological applications of QDs as fluorescent probes in biological imaging,<sup>12,13</sup> tunable absorbers and emitters in nanoscale electronics,<sup>14</sup> and quantum dot lasers.<sup>15</sup> In addition,

attempts have been made to deeply understand geometries, electronic, and optical properties of CdSe clusters that are with or without additional coordination ligands based on ab initio quantum chemical methods.<sup>16–21</sup>

Eichkorn et al.<sup>16</sup> modeled ligand-coordinated CdSe clusters by DFT calculations at BP86/SVP level. Four low-lying excitations were additionally determined using the TDDFT calculations. However, the clusters examined were nonstoichiometric CdSe units because of the presence of ligands. In addition, some of those clusters had extra electric charges. Troparevski et al.<sup>18</sup> and Deglmann et al.<sup>19</sup> constructed CdSe clusters from the optimized fragments of bulk layers, which were obtained either from the local density approximation (LDA) followed by molecular dynamics calculations or from the BP86/SVP calculations only, respectively. Electronic excitations of these clusters were also computed using TDDFT. However, most structures of global energy minima in these papers<sup>18,19</sup> deviate from the wurtzite structure, thereby contradicting the experimental results of CdSe clusters that adopt the wurtzite symmetry.<sup>1,22</sup> Puzder et al.<sup>21</sup> investigated geometries of CdSe clusters

<sup>†</sup> National Institute of Advanced Industrial Science and Technology.

<sup>‡</sup> Tohoku University.

<sup>§</sup> Nagoya University.

- (1) Murray, C. B.; Kagan, C. R.; Bawendi, M. G. *Annu. Rev. Mater. Sci.* **2000**, *30*, 545.
- (2) Qu, L.; Peng, Z. A.; Peng, X. *Nano Lett.* **2001**, *1*, 333.
- (3) Peng, Z. A.; Peng, X. *J. Am. Chem. Soc.* **2001**, *123*, 183.
- (4) Nirmal, M.; Norris, D. J.; Kuno, M.; Bawendi, M. G.; Efros, A. L.; Rosen, M. *Phys. Rev. Lett.* **1995**, *75*, 3728.
- (5) Efros, A. L.; Rosen, M.; Kuno, M.; Nirmal, M.; Norris, D. J.; Bawendi, M. G. *Phys. Rev. B* **1996**, *54*, 4843.
- (6) Efros, A. L.; Rosen, M. *Annu. Rev. Mater. Sci.* **2000**, *30*, 475.
- (7) Talapin, D. V.; Rogach, A. L.; Shevchenko, E. V.; Kornowski, A.; Haase, M.; Weller, H. *J. Am. Chem. Soc.* **2002**, *124*, 5782.
- (8) Qu, L.; Peng, X. *J. Am. Chem. Soc.* **2002**, *124*, 2049.
- (9) Ebenstein, Y.; Mokari, T.; Banin, U. *Appl. Phys. Lett.* **2002**, *80*, 4033.
- (10) de Mello Donega, C.; Hickey, S. G.; Wuister, S. F.; Vanmaekelberg, D.; Meijerink, A. *J. Phys. Chem. B* **2003**, *107*, 489.
- (11) Fisher, B. R.; Eisler, H. J.; Stott, N. E.; Bawendi, M. G. *J. Phys. Chem. B* **2004**, *108*, 143.
- (12) Michalet, X.; Pinaud, F.; Lacoste, T. D.; Dahan, M.; Bruchez, M. P.; Alivisatos, A. P.; Weiss, S. *Single Mol.* **2001**, *2*, 261.
- (13) Bakalova, R.; Ohba, H.; Zhelev, Z.; Nagase, T.; Jose, R.; Ishikawa, M.; Baba, Y. *Nano Lett.* **2004**, *4*, 1567.
- (14) Schlamp, M. C.; Peng, X.; Alivisatos, A. P. *J. Appl. Phys.* **1997**, *82*, 5837.
- (15) Klimov, V. I.; Mikhailovsky, A. A.; Xu, S.; Malko, A.; Hollingsworth, J. A.; Leatherdale, C. A.; Eisler, H.-J.; Bawendi, M. G. *Science* **2000**, *290*, 314.

(16) Eichkorn, K.; Ahlrichs, R. *Chem. Phys. Lett.* **1998**, *288*, 235.

(17) Leung, K.; Whaley, K. B. *J. Chem. Phys.* **1999**, *110*, 11012.

(18) Troparevsky, M. C.; Chelikowsky, J. R. *J. Chem. Phys.* **2001**, *114*, 943.

(19) Deglmann, P.; Ahlrichs, R.; Tsereteli, K. *J. Chem. Phys.* **2002**, *116*, 1585.

(20) Troparevsky, M. C.; Kronik, L.; Chelikowsky, J. R. *J. Chem. Phys.* **2003**, *119*, 2284.

(21) Puzder, A.; Williamson, A. J.; Gygi, F.; Galli, G. *Phys. Rev. Lett.* **2004**, *92*, 217401.

with and without additional ligands at the LDA level. They found that CdSe clusters maintain wurtzite structure and relaxed from their equilibrium geometry irrespective of whether they are pure or ligand stabilized. This report allows one to model uncoordinated CdSe clusters, which consume less CPU time, and generalize the calculations for ligand-coordinated clusters. Note, however, that relaxations in geometry and bond lengths are not experimentally demonstrated as well as no attempt has been made to compare electronic properties of the clusters that they predicted to those of real clusters synthesized using colloidal schemes.

The previous studies<sup>18–22</sup> reported ab initio determination of geometry, electronic, and optical properties of CdSe clusters that are uncoordinated or ligand-coordinated. Note that diameters of CdSe clusters are well documented<sup>23</sup> as a function of the first exciton peak position in experimental absorption spectra. However, no attempt is undertaken to compare the diameters of clusters that are predicted by using ab initio methods and experimental results. Lack of such comparison led to inconsistent conclusions. Bullen et al.<sup>24</sup> recently reported nucleation, growth, and subsequent determination of surface energy and initial size distribution of CdSe clusters in octadecene at  $\sim 270$  °C. They estimated from time-course of growth curve, concentration of initial precursors, and concentration of precursors left in equilibrium after growth process that a typical CdSe cluster of  $\sim 2$  nm in diameter consists of  $\sim 75$  CdSe molecules. In contrast, Soloviev et al.<sup>25</sup> estimated from absorption spectra and low temperature ( $\sim 4$  K) photoluminescence excitation (PLE) spectra of phenyl- and propyl-stabilized nonstoichiometric CdSe clusters that a  $\sim 2$  nm in diameter cluster consists of 32 stoichiometric CdSe units. This difference between  $\sim 75$  and  $\sim 32$  molecules arises because no attempt has been made in the past to know the exact geometry of a CdSe cluster that absorbs or emits at a particular wavelength window. To design nanoscale electronic devices using CdSe clusters, physically realistic structures and corresponding properties should be clearly understood.

In the present paper, we correlate the geometry of CdSe clusters with their optical properties using experimental absorption, PL, and XRD spectra as well as ab initio DFT calculations. CdSe clusters was nucleated and grown here from solutions containing cadmium oleate, trioctylphosphine selenium (TOPSe), trioctylphosphine (TOP), trioctylphosphine oxide (TOPO), and hexadecylamine (HDA) at 120, 150, and 180 °C. This synthesis scheme provided size-controlled luminescent CdSe clusters with  $\Phi_{\text{PL}}$  of 0.5 or larger. A change in the Cd–Se bond length of small clusters ( $\sim 2$  nm in diameter) from that in the bulk wurtzite was experimentally identified using Rietveld analysis of powder CdSe XRD spectrum. Using an approach to identify whether a proposed cluster is more physically reasonable, we developed cluster models ranging from three CdSe units to a cluster of mean diameter of  $\sim 2$  nm. Ab initio DFT calculations and experimental spectra were combined to show that a nucleus for the growth of a CdSe cluster has (CdSe)<sub>3</sub> stoichiometry with a six-membered ring structure in which Cd and Se atoms are located at the corners of an equilateral triangle. No PL was observed for (CdSe)<sub>3</sub>. Formation of the second cluster depends

on whether HDA was used in the growth solution. In the absence of HDA, the second cluster was (CdSe)<sub>6</sub>, which was characterized by a broad PL spectrum. No further growth occurred without HDA. On the other hand, in the presence of HDA, the second cluster was (CdSe)<sub>n</sub> (where  $n \geq 14$ ), which was characterized by a sharp PL spectrum. Further growth occurred with HDA depending on the reaction temperature and duration time. The surface energy of highly luminescent CdSe clusters synthesized through the current scheme with HDA was calculated as a function of temperature. The calculations show that the current synthesis scheme using HDA reduced agglomeration of clusters during nucleation and growth, thereby enhancing  $\Phi_{\text{PL}}$ .

## Experimental Section

We used cadmium oxide (95%, catalog number 031-00212, Wako, Tokyo), selenium shots (99.99%, catalog number 20 964-3, Aldrich, Tokyo), TOP (97%, Lot GBFA 005855, Lancaster, England), TOPO (90%, catalog number 346-02772, Wako, Tokyo), hexadecylamine (HDA, purity not available, catalog number 038-07612, Wako, Tokyo), and oleic acid (80%, catalog number 158-02391, Wako, Tokyo) as starting chemicals. Initially, a stock solution of TOPSe was prepared by dissolving selenium shots (2.694 g; 34.12 mmol) in TOP (25 mL) at 100 °C for 2 h in argon atmosphere, and then cooling them to room temperature (23 °C), thus producing 1.36 M stock solution. Therefore, 1 mL of stock solution contains 1.36 mmol of Se, which in turn is composed of 1 mL of TOP and 0.1078 g of Se. Next, a stock solution of cadmium oleate was prepared by dissolving CdO (10 g, 77.88 mmol) in oleic acid (65 mL) at 200 °C for 2 h, and then cooling to room temperature, thus producing 1.20 M stock solution. Therefore, 1.14 mL of cadmium oleate contains 1.36 mmol of Cd.

A typical synthesis route here is as follows: cadmium oleate (1.14 mL), TOP (2 mL), and TOPO (2 g) were simultaneously loaded in a three neck round-bottom flask (RB), melted, and degassed at  $\sim 100$  °C under alternate vacuum and argon for  $\sim 1$  h. Finally, the RB was filled with argon and placed in an oil bath kept at 120 °C for 10 min to attain thermal equilibrium. To the hot solution containing Cd precursor and coordinating solvents, 1 mL of TOPSe was quickly injected (injection time < 0.5 s). Nucleation and growth were allowed to take place at 120 °C. In the next synthesis, HDA (2 g) was also used together with cadmium oleate, TOP, and TOPO before injection of TOPSe. Syntheses were performed at 120, 150, and 180 °C. The growth solution contained 1.36 mmol of Cd and Se precursors, 3 mL of TOP as a total, 2.33 mL of HDA (calculated using specific gravity of dodecylamine, 0.806 g/cm<sup>3</sup>), and 2.38 mL of TOPO (specific gravity of TOPO is 0.84 g/cm<sup>3</sup> at 61 °C). The total volume of the reaction mixture was 8.71 mL. Aliquots (10  $\mu$ L) were taken from the reaction vessel using a pipet and subsequently dissolved in chloroform (1 mL), which was then diluted to 5 mL. One milliliter of this diluted solution was used for absorption and PL spectroscopic measurements.

Nucleation and growth of CdSe clusters were followed by UV–vis absorption and PL spectrometries using a spectrophotometer (Hitachi, model U-4100, Tokyo) and a spectrofluorometer (Hitachi, model F-4500, Tokyo), respectively. Structures of CdSe clusters were determined by powder X-ray diffractometry using an X-ray diffractometer (Rigaku, model RINT 2100, Tokyo) employing nickel filtered Cu K $\alpha$  radiation. The XRD patterns were recorded at  $2\theta$  from 10° to 80° using a fixed time method with a sampling step of 0.02°. A sampling time of 20 s was given at each step, thereby recording the XRD pattern for  $\sim 20$  h.

DFT calculations were performed with the use of Becke's three parameter hybrid method with the Lee, Yang, and Parr (B3LYP) gradient corrected correlation functional<sup>26</sup> using the Gaussian 03 W

(22) Murray, C. B.; Norris, D. J.; Bawendi, M. G. *J. Am. Chem. Soc.* **1993**, *115*, 8706.

(23) Yu, W. W.; Qu, L.; Guo, W.; Peng, X. *Chem. Mater.* **2003**, *15*, 2854.

(24) Bullen, C. R.; Mulvaney, P. *Nano Lett.* **2004**, *4*, 2303.

(25) Soloviev, V. N.; Eichhofer, A.; Fenske, D.; Banin, U. *J. Am. Chem. Soc.* **2000**, *122*, 2673.

(26) (a) Becke, A. D. *Phys. Rev. A* **1988**, *38*, 3098. (b) Lee, C.; Yang, W.; Parr, R. G. *Phys. Rev. B* **1988**, *38*, 3098.

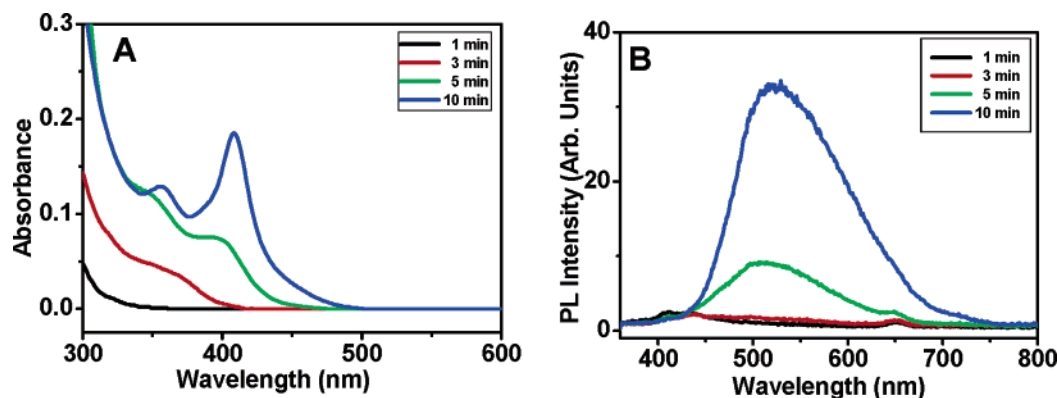


Figure 1. (A) UV–vis absorption and (B) PL spectra of CdSe clusters synthesized at 120 °C in the TOPO/TOP coordinating solvent system.

program packages.<sup>27</sup> Geometry optimizations were carried out using the standard double- $\zeta$  quality LanL2dz basis sets and followed by frequency calculations. Discrete spectra of excitation energies and corresponding oscillator strengths were obtained by the TDDFT method including  $n$  energy singlet transitions. Molecular volume of clusters was obtained using the PC Model program.

## Results and Discussion

**Nucleation and Growth of CdSe Clusters.** Figure 1 shows UV–vis absorption and PL spectra of aliquots taken from the growth mixture of cadmium oleate, TOP, TOPO, and TOPSe at 1, 3, 5, and 10 min at 120 °C. An excitonic transition at  $\sim 364$  nm was observed in the UV–vis absorption spectrum at 3 min, which was subsequently shifted to  $\sim 395$  nm at 5 min and to  $\sim 408$  nm at 10 min. The growth solution at 120 °C turned to turbid after 10 min, and no further growth was observed. No PL was detected up to 3 min, whereas a broad (fwhm  $\approx 150$  nm) PL was detected after 5 min.

In the next reaction, we added HDA in the growth mixture of cadmium oleate, TOP, and TOPO into which TOPSe was injected at temperatures  $\geq 120$  °C. Figure 2A and B shows UV–vis absorption and PL spectra of aliquots taken from the growth mixture at this fresh reaction at 1, 2, 4, 5, 10, and 15 min at 120 °C. Figure 2C and D shows UV–vis absorption and PL spectra corresponding to nucleation (1 min) and formation of the second cluster (2 min) at 150 °C. Also, Figure 2E and F shows UV–vis absorption and PL spectra corresponding to nucleation (0.2 min) and formation of the second cluster (1.0 min) at 180 °C. The reader may refer to the Supporting Information for complete UV–vis and PL spectra and time-course of growth estimated from absorption spectra at these temperatures. Similar to the reaction in the absence of HDA, an excitonic transition at  $\sim 364$  nm was observed at all three temperatures. No excitonic transition at the wavelength shorter than  $\sim 364$  nm was observed in the absorption spectra in Figures 1 and 2; therefore, the peak at  $\sim 364$  nm shows nucleation of CdSe clusters.

In the presence of HDA, nucleation was extended over a period of time. At 120 °C, nucleation continued until 10 min after injection of Se precursor, as shown in Figure 2A, together with enhancement in excitonic transition at  $\sim 364$  nm. Temporal extendibility of the nucleation was reduced with increasing processing temperature. At 150 °C, nucleation was completed in 1 min, whereas at 180 °C, nucleation was completed in 0.2

min. At all of these temperatures, nucleation is extended over a period of time, and the concentration of nuclei is increased before their growth into bigger sizes until a threshold concentration, similar to supersaturation, is reached. Once a supersaturation of nucleus is reached, the second cluster is formed. The second cluster showed an excitonic transition at  $\sim 427$ ,  $\sim 452$ , and  $\sim 489$  nm at 120, 150, and 180 °C, respectively. PL spectra of CdSe clusters synthesized with HDA were sharp (fwhm  $\approx 30$  nm), as compared to the PL spectrum of CdSe clusters that are synthesized without HDA (fwhm  $\approx 150$  nm). A weak deep trap PL was overlapped with the second cluster at 120 and 150 °C, which was reduced upon prolongation of the reaction time (see Supporting Information).

**Structural Characterization of CdSe Clusters.** Figure 3 shows the XRD pattern of CdSe clusters synthesized with HDA at 120 °C for 180 min. This pattern was fitted to wurtzite CdSe structure using the Le Bail algorithm for Rietveld refinement employed in the PowderCell 2.4 program.<sup>28</sup> The size of the cluster used for XRD measurement was found to be 2.02 nm from absorption spectra. The crystallographic information file (CIF) of bulk CdSe<sup>29</sup> was used for the Le Bail fitting. Residues of fitting were  $R_p = 12.49$ ,  $R_{wp} = 16.50$ , and  $R_e = 12.51$ , where symbols have their usual meanings.<sup>30</sup> The “goodness of fit indicator” calculated from the residues was 1.32, which indicates that the current fitted atomic positions and lattice parameters that will be discussed below are acceptable.<sup>30</sup>

In bulk wurtzite CdSe, Cd and Se atoms occupy 2b positions at  $(1/3, 2/3, 0)$  and  $(1/3, 2/3, 0.376)$ , respectively.<sup>29</sup> These atomic positions gave two equilibrium Cd–Se bond lengths, 0.2631 and 0.2635 nm. Lattice parameters of bulk wurtzite CdSe are  $a = b = 0.4229$  nm;  $c = 0.7010$  nm;  $\alpha = \beta = 90^\circ$ ;  $\gamma = 120^\circ$ .<sup>29</sup> The current XRD pattern fits well to the wurtzite structure, which can be readily seen from the “goodness of fit indicator”; that is, bulk wurtzite symmetry is retained in the current  $\sim 2$  nm CdSe clusters. However, both atomic positions and lattice parameters of CdSe clusters are displaced from the bulk geometry. The refinable atomic parameter of wurtzite CdSe is the  $z$ -coordinate. The  $z$ -coordinates of Cd and Se atoms are displaced from 0 to  $-0.0143$  and from 0.376 to 0.362, respectively. Correspondingly, Cd–Se bond lengths are changed from 0.2631 to 0.2668 nm and from 0.2635 to 0.2673 nm. These changes provoked an increase in the lattice parameters of the

(28) Kraus, W.; Nolze, G. *J. Appl. Crystallogr.* **1996**, *29*, 301.

(29) Stevenson, A. W.; Barnea, Z. *Acta Crystallogr.* **1984**, *B40*, 530.

(30) Young, R. A. *The Rietveld Method*; International Union of Crystallography/Oxford University Press: Oxford, 2002.

(27) Frisch, M. J.; et al. *Gaussian 03*, revision C02; Gaussian, Inc.: Wallingford, CT, 2004.



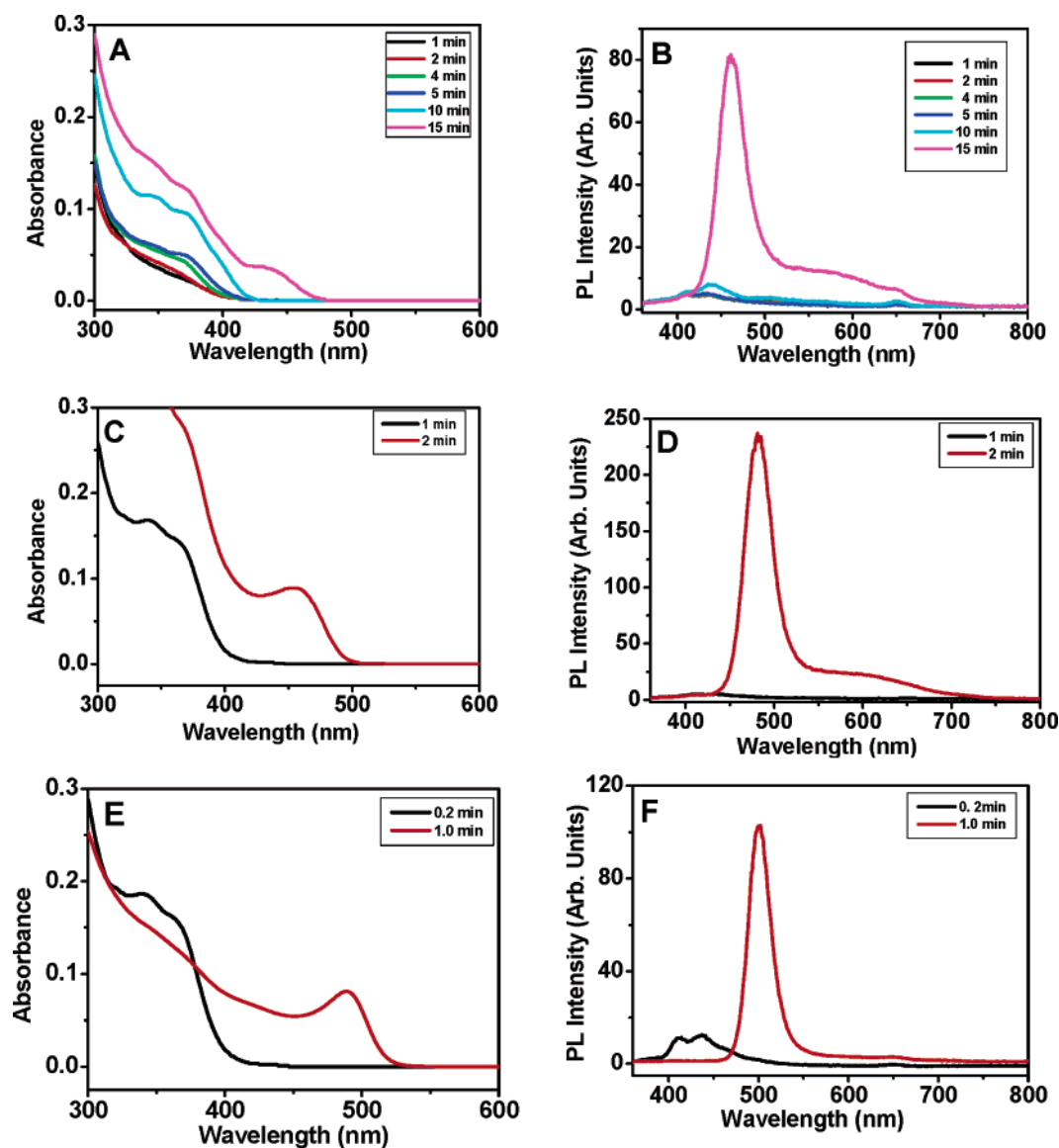


**Figure 2.** (A) UV-vis absorption and (B) PL spectra of CdSe clusters synthesized at 120 °C in the TOPO/TOP/HDA coordinating solvent system. (C) and (D) are for corresponding spectra recorded at 150 °C, while (E) and (F) are for corresponding spectra recorded at 180 °C.

current  $\sim 2$  nm CdSe clusters. A change from  $a = b = 0.4229$  nm to  $a = b = 0.4361$  nm, and from  $c = 0.7010$  nm to  $c = 0.7110$  nm, was observed upon Rietveld analysis. Thus, we experimentally identify that equilibrium geometry of CdSe is changed when the cluster size is reduced below exciton Bohr radius. Note that the deviation of Cd–Se bond lengths from its bulk values detected by XRD is an averaged value. To determine deviation in the Cd–Se bond length of individual atomic pairs from that of bulk geometry, we investigated the structure and electronic properties of CdSe clusters using *ab initio* DFT methods.

**Structure–Property Relationship of CdSe Clusters Up to a Diameter of  $\sim 2$  nm.** We now discuss structures of CdSe clusters determined by *ab initio* DFT calculations and then compare calculated discrete electronic spectra with those observed experimentally. Here, we should remind that CdSe clusters of various size and morphology are determined at different levels of *ab initio* methods.<sup>16–21</sup> However, no attempts have been made in previous works to examine whether a proposed cluster model is really formed in any colloidal growth

conditions or not. In our study, we examined whether a cluster model is applicable to the real colloidal growth described in the section Nucleation and Growth of CdSe clusters.

Initially, the geometries of hexagonally stacked clusters were optimized using the conventional energy minimization technique that was followed by harmonic frequency calculations and analysis of their IR spectra (data not shown). No imaginary frequencies were observed in the IR spectrum for all of the clusters discussed here. Next, oscillator strengths ( $f$ ) of discrete electronic spectra that consist of the first few dozens of singlet states were calculated using the TDDFT technique. The oscillator strengths thus calculated were classified into three categories, that is, “high” ( $f > 0.06$ ), “low” ( $f < 0.02$ ), and “intermediate” ( $0.02 < f < 0.06$ ). The next step was to determine the HOMO–LUMO energy gap from the calculated spectrum. Toward this aim, we first determined the diameter of the cluster from its molecular volume and then calculated the wavelength of excitonic transitions using the empirical nonlinear dependence of the diameter of a given CdSe sample on the wavelength of its first excitonic absorption peak compiled by Yu et al.<sup>23</sup> Next,

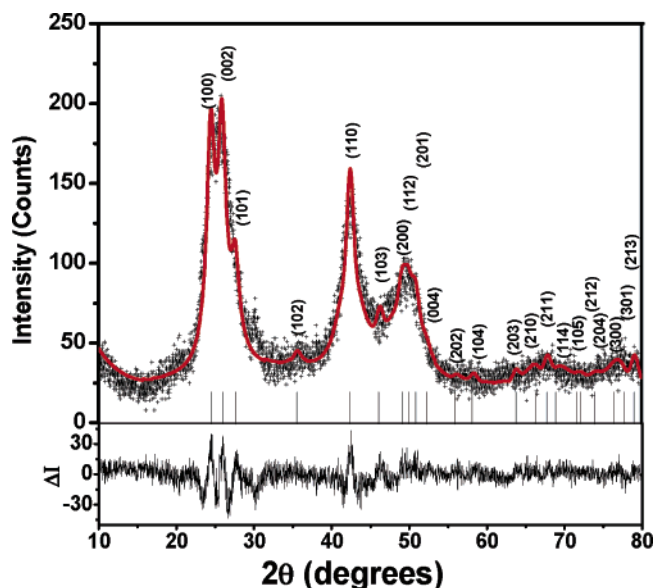


**Figure 3.** Rietveld refinement plot for CdSe clusters. The experimental and simulated intensity data ( $I_e$  and  $I_s$ ) are plotted as plus signs (+) and red solid lines, respectively, and  $\Delta I = I_e - I_s$  below. The tick marks indicate the position of all possible Bragg reflections from the CIF file obtained from the Inorganic Crystal Structure database Collection Code 60630.

we examined whether electronic transitions corresponding to the wavelength obtained from the above empirical curve are present in the calculated spectrum. If present, we further examined whether we have two identical oscillator strengths that are closely separated ( $\leq 3$  meV) in the calculated spectrum. A reason for this examination is the fact that an exciton in a semiconductor cluster has two possible states: one is dark and the other is bright, which are split into two energies by electron–hole exchange interaction. If two oscillator strengths are found, they are assigned to HOMO–LUMO transitions: one is the bright and the other is the dark. If no such fine structure is found in oscillator strengths, the cluster model is discarded at this stage, and we move on to searching for alternative structures that meet the above criterion of dark and bright exciton. To examine whether such a physically significant cluster is formed under the current synthetic scheme, we compared the experimental absorption spectra (see Figures 1 and 2) to the theoretically predicted absorption spectra. An agreement in diameters determined by ab initio DFT calculations and from experimental absorption spectra was a prerequisite for a comparison between the calculated and experimental spectra.<sup>31</sup>

Figure 4 shows optimized geometries of  $(\text{CdSe})_n$  ( $n \geq 3$ ), where the suffix  $n$  denotes the number of CdSe molecular units. Figure 4A shows the optimized structure of  $(\text{CdSe})_3$ , which is reported as a structure of global minimum for CdSe trimers.<sup>18,19</sup> Furthermore, a trimer is the first real building unit of hexagonal crystal structure.<sup>19</sup> The  $(\text{CdSe})_3$  has  $C_{2V}$  symmetry with a six-membered ring structure. Both Cd and Se atoms in  $(\text{CdSe})_3$  are 2-fold coordinated (2C). The optimized Cd–Se bond length in  $(\text{CdSe})_3$  is 0.2597 nm, which is shorter than equilibrium Cd–Se bond lengths of bulk wurtzite CdSe, that is, 0.2631 and

0.2635 nm.<sup>29</sup> The diameter of  $(\text{CdSe})_3$  determined from its molecular volume is 1.20 nm, which exactly matches the size determined from the experimental UV–vis absorption spectrum (1.20 nm) recorded at 10 min and at 120 °C (see Figure 2A). Figure 5A shows the calculated absorption spectrum of  $(\text{CdSe})_3$ , which is compared to the above UV–vis absorption spectrum. The electronic transition centered at  $\sim 364$  nm is assigned to the HOMO–LUMO gap because the empirical curve of Yu et al.<sup>23</sup> gave a diameter of 1.20 nm for  $\sim 364$  nm. The transition centered at  $\sim 364$  nm is a doublet with a separation of 2.8 meV whose intensity (or oscillator strength) differs by only  $2 \times 10^{-4}$  au. This fine structure in the calculated spectra indicates that the transition at  $\sim 364$  nm corresponds to HOMO–LUMO. Figure 5A thus shows that the calculated discrete electronic transitions of  $(\text{CdSe})_3$  reproduce the experimental absorption spectrum of a CdSe nucleus. Therefore, we conclude that (i) the diameter of  $(\text{CdSe})_3$  estimated from the DFT calculations matches well with that determined from the experimental absorption spectra, (ii) the calculated HOMO–LUMO transition coincides with the experimental excitonic peak, and (iii) a fine structure was observed in the calculated spectra showing that  $(\text{CdSe})_3$  (Figure 4A) is the CdSe nucleus formed in the present reaction conditions. A red shifted “intermediate” oscillator strength from the HOMO–LUMO transition was observed in the calculated electronic spectrum of  $(\text{CdSe})_3$ . This transition is attributed to a surface atomic state that arises from coordinatively unsaturated sites.<sup>17,20</sup>

Figure 4B shows the optimized geometry of  $(\text{CdSe})_6$ , which is the smallest wurtzite cage with  $C_1$  symmetry. This geometry is obtained from an antiparallel stacking of the two  $(\text{CdSe})_3$  layers. However, unlike  $(\text{CdSe})_3$ ,  $(\text{CdSe})_6$  has only 3C for all sites, although all three bond lengths for a distinct atom differ slightly. The Cd–Se bond lengths varied from 0.2698 to 0.2863 nm. An increase in the bond length for 3C sites as compared to that for 2C sites is due to the fact that Cd atoms form  $sp^2$  hybridization with the three nearest Se atoms, thereby exhibiting bond lengths similar to those of bulk CdSe.<sup>21</sup> The diameter of  $(\text{CdSe})_6$  determined from its molecular volume is 1.50 nm, which matches with the diameter determined from the experimental UV–vis absorption spectra (1.58 nm) at 5 min and at 120 °C in the absence of HDA (see Figure 1A). However, no absorption spectrum was recorded in the presence of HDA that gave a spectrally estimated diameter of 1.50 nm, which means that coordinating solvents play a significant role in the evolution of CdSe clusters. Figure 5B compares the calculated absorption spectrum of  $(\text{CdSe})_6$  with the UV–vis absorption spectrum at 5 min and at 120 °C in the absence of HDA. A transition at  $\sim 395$  nm is assigned to the HOMO–LUMO gap because the empirical curve of Yu et al.<sup>23</sup> gave a diameter of 1.58 nm for this wavelength. Similar to  $(\text{CdSe})_3$ , the transition at  $\sim 395$  nm is a doublet with a separation of 0.6 meV. The magnitude of the doublet transitions differs by  $4 \times 10^{-4}$  au. Thus, we conclude that  $(\text{CdSe})_6$  is the second cluster formed in the synthetic scheme without using HDA. The  $(\text{CdSe})_6$  is characterized by a broad PL spectrum (see Figure 1B), which most likely arises from an “intermediate” oscillator strength at  $\sim 376$  nm.<sup>17,20</sup>

Figure 4C shows the optimized geometry of  $(\text{CdSe})_{13}$ , which can be described as a stacked structure of the two layers of the three fused hexagonal rings. All atoms in  $(\text{CdSe})_{13}$  are 3C like  $(\text{CdSe})_6$ , whose bond length varies from 0.2648 to 0.2802 nm.

(31) Hereafter, we refer to molecular diameters determined from molecular volumes using the PC Model program. It calculates analytically using the algorithms proposed in the literature.<sup>32</sup> Note that molecular volume is a fundamental physical property of molecules so that proper determination is important to understand their structure, function, and interactions. Moreover, molecular diameters thus obtained cannot be compared literally to those defined from internuclear distances.<sup>32</sup>

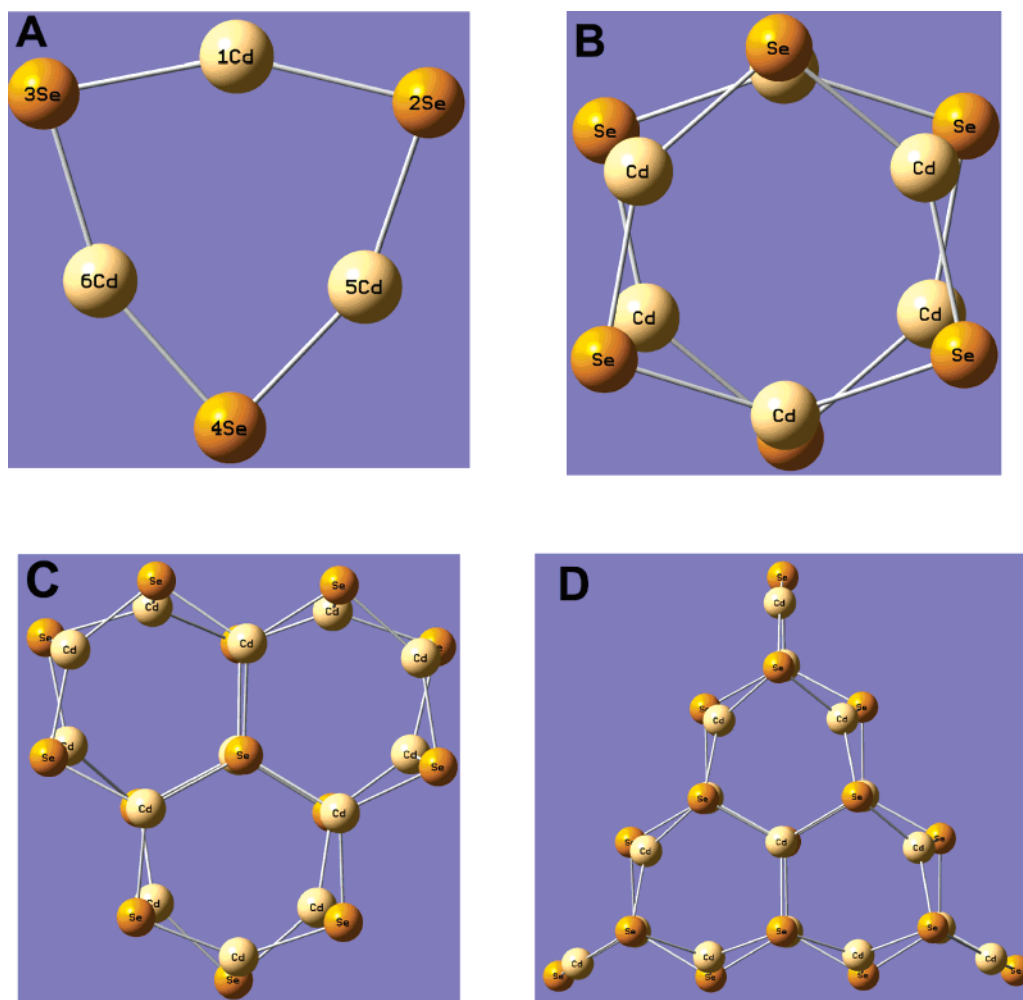


**Figure 4.** Optimized geometries for (A)  $(\text{CdSe})_3$ , (B)  $(\text{CdSe})_6$ , (C)  $(\text{CdSe})_{13}$ , and (D)  $(\text{CdSe})_{16}$ .

The diameter of  $(\text{CdSe})_{13}$  calculated from its molecular volume is 1.90 nm, which shows 10% deviation from the diameter estimated from the UV–vis absorption spectrum recorded at 10 min at 120 °C (1.64 nm). Figure 5C compares the calculated absorption spectrum of  $(\text{CdSe})_{13}$  with the UV–vis absorption spectrum at 10 min in the absence of HDA (Figure 1A). Electronic transitions centered at  $\sim 410$  nm are assigned to the HOMO–LUMO gap because the empirical curve of Yu et al.<sup>23</sup> gave a diameter 1.64 nm for this wavelength, which exactly matches with the experimentally determined diameter. These two transitions have a separation of 0.3 meV. The magnitude of doublet transitions differs by  $1 \times 10^{-4}$  au. Figure 5C thus clearly shows that the calculated absorption spectrum of  $(\text{CdSe})_{13}$  reproduces the experimental absorption spectrum, although its molecular diameter deviates from the experimental diameter.

Note that the above-discussed clusters  $(\text{CdSe})_3$ ,  $(\text{CdSe})_6$ , and  $(\text{CdSe})_{13}$  show either no PL or a broad PL (see Figure 1B). Remember that either  $(\text{CdSe})_6$  or  $(\text{CdSe})_{13}$  is not formed when HDA was also included as a coordinating solvent. The second cluster formed at 120 °C in the presence of HDA showed an electric transition at  $\sim 427$  nm (at 120 °C). This transition was shifted to longer wavelengths as the reaction temperature was increased from 120 °C to 150 and 180 °C. The cluster formed was characterized by sharp PL with  $\Phi_{\text{PL}} \approx 0.30$  that increased to  $\sim 0.50$  upon prolongation of the reaction time. Among many

clusters theoretically considered,  $(\text{CdSe})_{16}$  is best fitted to explain the experimental observation of the 2-min absorption spectrum at 150 °C in Figure 2C. The  $(\text{CdSe})_{16}$  cluster was obtained by the addition of an extra 3 units of CdSe to the  $(\text{CdSe})_{13}$  cluster. Figure 4D shows the optimized geometry of  $(\text{CdSe})_{16}$ . In the  $(\text{CdSe})_{16}$  cluster, we have three pairs of 2C sites out of 32 atoms. Unlike  $(\text{CdSe})_3$ , the Cd–Se bond length of 2C sites (0.2642 nm) is longer than that in bulk (0.2631 nm). The diameter of  $(\text{CdSe})_{16}$  determined from its molecular volume is 2.02 nm, which is close to that determined from the experimental UV–vis absorption spectrum at 30 min (2.01 nm) after injection of TOPSe (see Figure S1A in the Supporting Information). Figure 5D shows the calculated spectrum of  $(\text{CdSe})_{16}$  as compared to the experimental UV–vis absorption spectrum at 2 min and at 150 °C. Electronic transitions around  $\sim 463$  nm are assigned to HOMO–LUMO; the empirical curve reported by Yu et al.<sup>23</sup> gave a diameter of 2.05 nm for this wavelength. These two transitions have a separation of 0.1 meV. The magnitude of doublet transitions differs by  $1.1 \times 10^{-3}$  au. Thus, we conclude that the formation of  $(\text{CdSe})_{16}$  is more physically reasonable under the present growth conditions.

Finally, it is worth noting that the TDDFT method applied here is one of the best and superior methods for calculating excitation energies of complex molecules and becomes very popular for describing spectroscopic properties of various bulk solids, clusters, nanoparticles, and nanostructures as well as

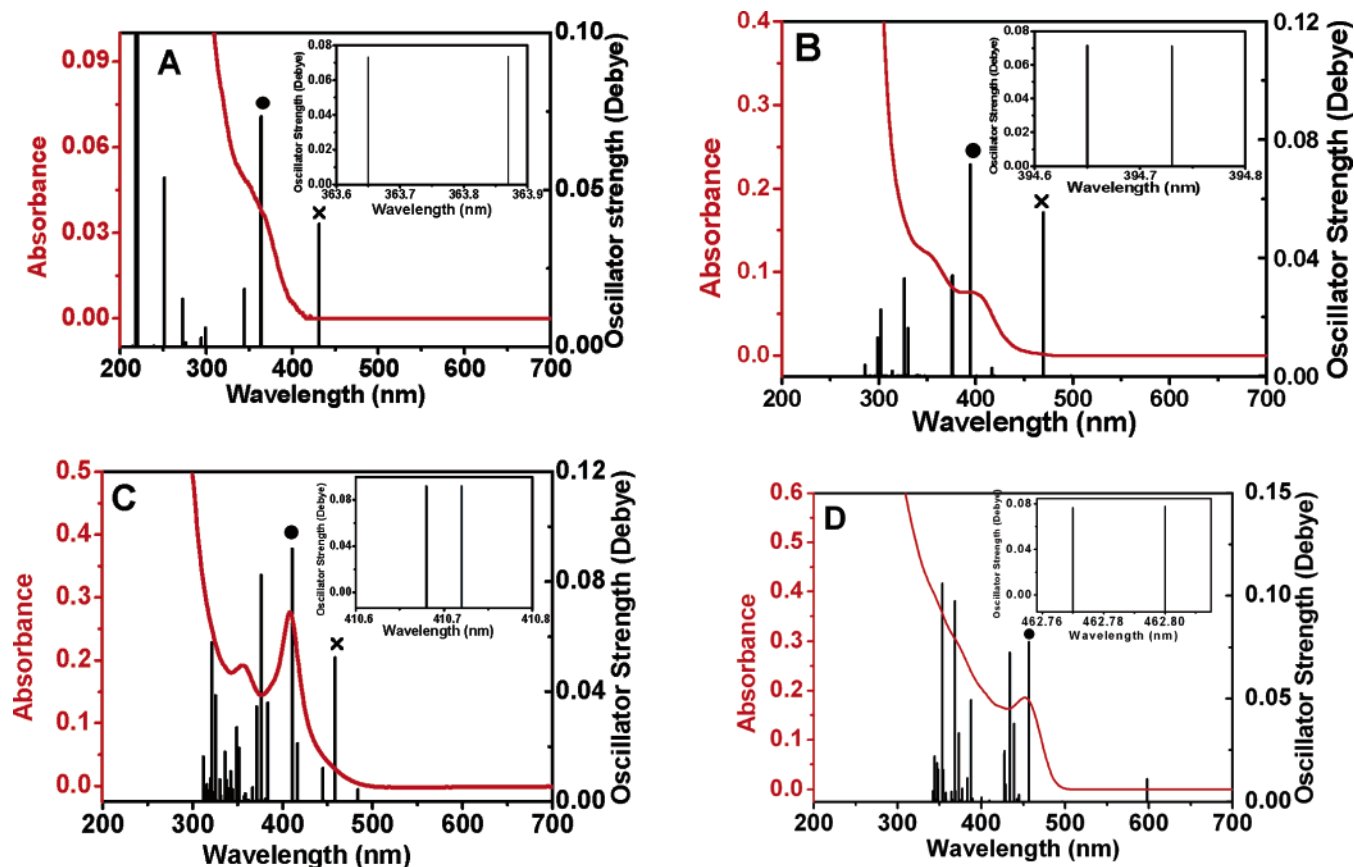


**Figure 5.** Comparison of the calculated transition oscillator strengths and experimental UV–vis absorption spectra of (A)  $(\text{CdSe})_3$ , (B)  $(\text{CdSe})_6$ , (C)  $(\text{CdSe})_{13}$ , and (D)  $(\text{CdSe})_{16}$  clusters. The first three experimental absorption spectra were recorded at (A) 2 min, (B) 5 min, and (C) 10 min after starting the reaction using the TOPO/TOP coordinating solvent system, while (D) is for the TOPO/TOP/HDA coordinating solvent containing system recorded at 2 min and 150 °C. The oscillator strengths marked with “●” are HOMO–LUMO transitions, while those with “x” arise from surface trap. Inset of each figure: A magnified view of the electronic transitions assigned to HOMO–LUMO.

several fundamental biological processes. For about two decades, this cost effective method proved extremely interesting as a predictive tool in describing related phenomena. The main point in our present study is the minimal CdSe unit size necessary to be considered as building blocks to follow the observed experimental findings. Keeping the symmetry as well as wurtzite structure motif, we have found that  $(\text{CdSe})_3$  is the mean target structure. On the basis of this structure, one can obtain those four distinct structures that describe our above experimental findings. Because of the presence of a large number of 2-fold coordinated sites for the  $(\text{CdSe})_n$  where  $n \leq 14$ , these sites effectively diminished by self-coordination to the next nearest centers via strong distortion of the initial structure symmetry as can be seen in Figure 4B and C. Thus, for example, for  $(\text{CdSe})_n$  where  $n \leq 14$ , all centers are 3-fold coordinated despite the initial three pairs of 2-fold coordinated sites. However, for the  $(\text{CdSe})_{16}$  cluster, the latter three pairs are well separated and can be considered as a highly stable unit to describe the observed differences in our PL spectra.

We should also note that our theoretical considerations are based on the gas-phase cluster calculations despite the experiments carried out on colloidal solutions. However, this is not new methodology but a well-accepted recipe as is widely applied in the zeolite chemistry and catalysis.<sup>33</sup> Evidently, the latter highly strong structure-directing solvents can modify to some

extent the structure of those considered CdSe clusters by molecular coordination to many Lewis acid sites of QDs. Fortunately, because of well separation of absorption bands for those considered amines, phosphines, and other solvents used here (they appeared far below at about 200 nm) from those of the isolated  $(\text{CdSe})_n$  clusters, they were not expected to strongly shift the absorption bands observed and discussed here in the present study.

To further support the latter issue, we have additionally performed theoretical calculations at the same TDDFT//B3LYP/Lan12dz level that model the interaction of the selected solvent molecules with the smallest  $(\text{CdSe})_3$  and the largest  $(\text{CdSe})_{16}$  clusters and their respective absorption spectra. Note that in these calculations the TOP, TOPO, and HDA were replaced by triethylphosphine (TEP), triethylphosphine oxide (TEPO), and monoethylamine (MEA), respectively, with the aim to decrease the CPU time. The optimized geometries of these adsorption complexes were tabulated and can be obtained from the authors at request. Table 1 shows the results of these calculations and the main characteristics of the adsorption complexes thus obtained. It is clear that the interaction of TEPO is twice as strong as that of TEP with both the smallest and the largest cluster models. Most important is, however, that the coordination

(32) Connolly, M. L. *J. Am. Chem. Soc.* **1985**, *107*, 1118.

(33) (a) Sauer, J.; Ugliengo, P.; Garrone, E.; Saunders, V. R. *Chem. Rev.* **1994**, *94*, 2095. (b) Zhanpeisov, N. U.; Anpo, M. *J. Am. Chem. Soc.* **2004**, *126*, 9439. (c) Zhanpeisov, N. U.; Matsuoka, M.; Yamashita, H.; Anpo, M. *J. Phys. Chem. B* **1998**, *102*, 6915.



**Table 1.** Bond Distance (Cd–X, in Å) between the Closest Atom X and the Surface Cd Atom, Where X = P (for TEP), O (for TEPO), and N (for MEA), Adsorption Energy ( $E_{\text{ads}}$ , in kcal/mol), Wavelength ( $\lambda$ , in nm), and Excitation Energy ( $E_{\text{exc}}$ , in eV) for the Adsorption Complexes of TEP, TEPO, and MEA with (CdSe)<sub>3</sub> and (CdSe)<sub>16</sub> Cluster Models

property	(CdSe) <sub>3</sub>		(CdSe) <sub>16</sub>		
	TEP	TEPO	TEP	TEPO	MEA
Cd–X	2.859	2.201	2.970	2.202	2.511
$E_{\text{ads}}$	17.8	32.0	19.4	35.3	20.8
$\lambda$	359	363	463	465	461
$E_{\text{exc}}$	3.45	3.41	2.68	2.66	2.69

of either TEP or TEPO did not strongly shift the target absorption band centered at around 364 nm observed for the isolated (CdSe)<sub>3</sub> cluster (see Table 1). Similar results were also obtained for the largest (CdSe)<sub>16</sub> cluster model when considering the adsorption complexes with TEP, TEPO, and MEA. Thus, the theoretical results for the isolated cluster models are indispensable to clarify the origin of bands and to assign them to reliable cluster models in parallel experiments.

**Surface Energy of Small CdSe Clusters.** The surface energy  $E_{\text{S}}$  of colloidal clusters is given by

$$E_{\text{S}} = (r_{\text{nuc}}/4V_{\text{m}})RT \ln S_{\text{t}} \quad (1)$$

Here,  $r_{\text{nuc}}$  is the radius of a nucleus,  $V_{\text{m}}$  is the molar volume of the material, and  $S_{\text{t}}$  is a dimensionless parameter describing oversaturation of precursors in the solution during nucleation.<sup>34</sup> In the above equation, the unknown parameters are  $r_{\text{nuc}}$  and  $S_{\text{t}}$ . Our low-temperature reactions and subsequent structure–property determination considerably simplify the situation. The nucleus of CdSe clusters formed at all three temperatures at which the reaction is carried out has a (CdSe)<sub>3</sub> stoichiometry and 1.20 nm diameter. Bullen et al.<sup>24</sup> recently reported a procedure to determine the surface energy of colloidal CdSe clusters by employing a time-course of the growth curve and size-dependent molar absorption coefficients reported by Yu et al.<sup>23</sup> In this report,  $r_{\text{nuc}}$  is determined by extrapolating the time-course of growth curve at the time of injection.<sup>24</sup> However, it raises severe limitations on the accuracy of determination of diameter and number of molecular units present in a cluster. In contrast to this, in our report we have simulated structures of CdSe clusters by ab initio DFT calculations, thereby allowing one to find out the exact nucleus diameter and number of molecules constituting the cluster. The degree of supersaturation  $S_{\text{t}}$  can be estimated if the residual concentration of precursors immediately after the nucleation is known. The procedure to determine  $S_{\text{t}}$  from initial precursor concentration, number of

molecules in a nucleus, and concentration of CdSe during nucleation is explained in Bullen et al.<sup>24</sup> We calculate  $E_{\text{S}}$  as 28.67, 43.34, and 59.88 mJ/m<sup>2</sup> at 120, 150, and 180 °C, respectively. Note that the surface energy of CdSe clusters synthesized in the current coordinating solvent systems is an order of magnitude smaller than that of CdSe clusters synthesized using octadecene. Reduced surface energy lowers the agglomeration of clusters that is responsible for the high  $\Phi_{\text{PL}}$  of CdSe clusters synthesized by using our present synthesis scheme.

## Conclusions

In conclusion, structure and properties of CdSe clusters up to a mean diameter of ~2 nm are established using experimental UV–vis absorption and PL spectra, and TDDFT calculations. CdSe clusters for the present study were nucleated and grown from a solution containing cadmium oleate, TOPSe, HDA, TOP, and TOPO at three temperatures, 120, 150, and 180 °C, following the hot-injection technique. This synthetic scheme provided size-controlled CdSe clusters having  $\Phi_{\text{PL}}$  up to 0.5. Rietveld analysis of experimental XRD pattern proved that Cd–Se bond lengths of CdSe clusters up to ~2 nm in diameter deviate from its bulk equilibrium bond length. Experimental spectra and ab initio calculations were combined to show that the nucleus of a CdSe cluster has a (CdSe)<sub>3</sub> stoichiometry and has a six-membered ring structure in which Cd and Se atoms are located at the corners of an equilateral triangle. No PL was observed for (CdSe)<sub>3</sub>. The formation of the second cluster depended on whether HDA was used in the growth solution. In the absence of HDA, the second cluster was (CdSe)<sub>6</sub>, which was characterized by a broad PL spectrum, whereas in the presence of HDA, the second cluster was (CdSe)<sub>n</sub> ( $n \geq 14$ ), which is characterized by a sharp PL spectrum. Surface energy of luminescent CdSe clusters synthesized using TOPO/TOP/HDA coordinating solvents as a function of temperature is calculated. Surface energy is found to be an order of magnitude less than that of CdSe clusters synthesized using octadecene at 275 °C, which shows that the current synthetic scheme reduced agglomeration of clusters during nucleation and growth due to a lower value of surface energy, which thereby enhances  $\Phi_{\text{PL}}$ .

**Acknowledgment.** N.U.Z. and H.F. would like to acknowledge the Grant-in-Aid support from the Ministry of Education, Science, and Culture of Japan (16072203).

**Supporting Information Available:** Complete bibliographical details of ref 27. UV–vis absorption and PL spectra at 120, 150, and 180 °C. Time-course of growth curve at 120, 150, and 180 °C. This material is available free of charge via the Internet at <http://pubs.acs.org>.

JA0565018

(34) Talapin, D. V.; Rogach, A. L.; Haase, M.; Weller, H. *J. Phys. Chem. B* **2001**, *105*, 12278.